Russian Journal of Applied Chemistry, Vol. 76, No. 6, 2003, pp. 989–996. Translated from Zhurnal Prikladnoi Khimii, Vol. 76, No. 6, 2003, pp. 1017–1024.

MACROMOLECULAR CHEMISTRY AND POLYMERIC MATERIALS

Structural Parameters of Cellulose Produced by *Acetobacter Xylinum* and Their Variation in the Course of Drying of Gel Films

Yu. G. Baklagina, A. K. Khripunov, A. A. Tkachenko, S. V. Gladchenko, V. K. Lavrent'ev, A. Ya. Volkov, V. K. Nilova, V. M. Denisov, T. E. Sukhanova, I. S. Zanaveskina, V. V. Klechkovskaya, and L. A. Feigin

Institute of Macromolecular Compounds, Russian Academy of Sciences, St. Petersburg, Russia

St. Petersburg State University, St. Petersburg, Russia

Institute of Cytology, Russian Academy of Sciences, St. Petersburg, Russia

Institute of Crystallography, Russian Academy of Sciences, Moscow, Russia

Received March 14, 2003

Abstract—The cellulose-producing power of the VKM V-800 *Acetobacter xylinum* strain under conditions of static culture was studied. The culture medium was optimized with the aim to increase the cellulose yield and obtain highly crystalline cellulose I with molecular weight of about 5×10^5.

A considerable progress in studies of cellulose biosynthesis, development of the concepts of structural hierarchy of cellulose, and discovery of two crystalline modifications, CI_α and CI_β, in native cellulose samples stimulated in the past decade active studies of evolutionarily different celluloses on the molecular and supramolecular levels. The structure of native celluloses is extensively studied by biochemical, genetic, physicochemical, and also theoretical methods [1–12].

The most success has been gained in studies of cellulose produced by *Valonia ventricosa* alga and of bacterial cellulose produced by *Acetobacter xylinum* (CAX) [3].

Two polymorph families of crystalline cellulose I are distinguished: that rich in the I_α form (algal and bacterial celluloses) and that rich in the I_β form (cellulose of higher plants and animal cellulose) [7–10]. Electron diffraction studies showed that, in the metastable I_α phase, cellulose chains are packed to form a triclinic cell (space group $P1$) with a single tie chain, and under certain conditions, this phase transforms into the thermodynamically stable monoclinic I_β structure (space group $P2_1$) with two macrochains in the unit cell [7, 10]. The I_α/I_β ratio for celluloses of various origins forms in the course of biosynthesis and is not directly related to the degree of crystallinity of a polymeric sample. For example, in the cellulose produced by *Valonia ventricosa* alga (degree of crystallinity 100%) I_α/I_β = 60/40, and in the animal cellulose produced by *Halocynthia*, with the same degree of crystallinity, this ratio is 10/90 [12].

It has been found [9] that the degree of transformation of structures I_a and I_b during heat treatment of cellulose samples is independent of the initial crystallinity. In this context, a fundamental question arises concerning exact ultrastructural localization of each phase. This question was answered to certain extent in recent papers [13, 14]; the procedure used was based on different reactivities of the I_α and I_β phases. The conclusion of [13, 14] that the I_α phase is situated on the surface of microcrystals or microfibrils was also confirmed by the data of high-resolution atomic-force microscopy [15].

Numerous papers published in the past five years show that the ratio and sizes of structural modifications I_α and I_β and their mutual arrangement depend both on the evolutionary origin of cellulose samples and on the biosynthesis conditions, varying from one sample to another [16].

The efforts of many research teams are aimed today at revealing the factors responsible for variation of the I_α/I_β ratio in the course of cellulose biosynthesis.

1070-4272/03/7606-0989 $25.00 © 2003 MAIK "Nauka/Interperiodica"

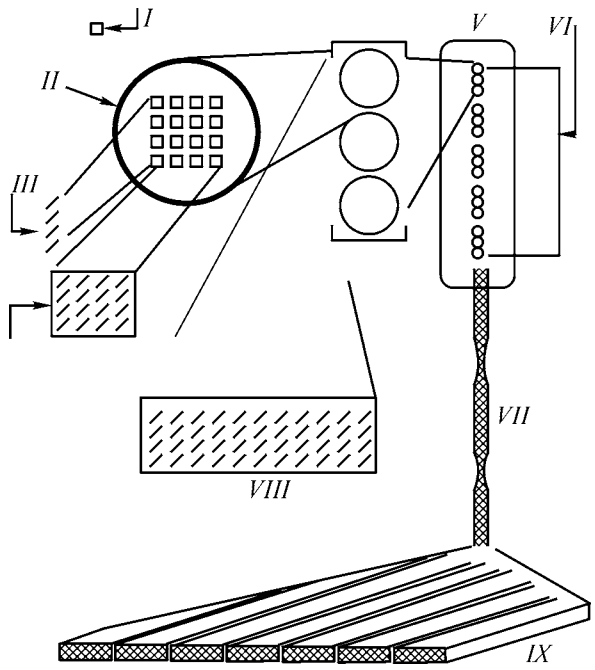

Fig. 1. Scheme of the structure of linear TC of *A. xylinum* bacterium, illustrating the formation of a mini-sheet from four glucan chains and of a mini-crystal from 16 chains by a subunit: (*I*) catalytic site of a glucan chain, (*II*) TC subunit, (*III*) mini-sheet, (*IV*) mini-crystal of one TC subunit, (*V*) TC triplet, (*VI*) linear series of Acetobacter TC triplets, (*VII*) ribbon of microfibrils, (*VIII*) crystalline microfibril of three TC subunits, and (*IX*) 10–100 microfibrils/ribbon. Three TC subunits form a crystalline microfibril, and 10–100 subunits form a ribbon.

Particular attention is given to crystallization of bacterial CAX as a model system for which the I_α/I_β ratio varies with strain and cultivation conditions (e.g., addition of chemicals to culture medium, variation of temperature) [3, 4, 16].

The interest in fine details of biosynthesis and structure of CAX is due to the possibility of preparing chemically pure cellulose by an environmentally acceptable procedure and using it in diverse branches of medicine [17] and engineering [18]. Various structural levels of CAX are discussed: the structure of the terminal complex (TC) itself; its subunit; fine structural elements formed: mini-sheet, mini-crystal, microfibril, and ribbon [3, 11]. Brown [3] suggested a scheme (Fig. 1) illustrating the shape and size of a linear TC and their correlation with the microfibril size. Each TC subunit includes 16 catalytic sites forming four mini-sheets, which, in turn, form a mini-crystal. A microfibril is formed from three TC subunits, and a ribbon, from 10–100 microfibrils. Experiments on CAX cultivation with addition of Tinopoal dye showed that the macrochain packing varies with dye concentration. At low dye concentrations, the microfibril formation is disturbed. At high dye concentrations, only mini-sheets of glucan chains are obtained in the form of tubular cellulose; in the course of washing or photoisomerization, this structure can transform into a microfibril [11].

Attempts are made to affect, via the composition of the culture medium, the capability of *A. xylinum* strains to produce ribbons and their aggregates with more perfect structural characteristics. It has been shown [19] that addition to the culture medium of antimetabolites, such as nalidixic acid and chloramphenicol, makes bacterial cells longer and, as a consequence, results in production of wider ribbon aggregates.

The effect of polymeric additives on the formation of CAX microfibrils of various sizes and the mechanism of crystallization of cellulose I_α and I_β in them are discussed in [20–22]. It was found that addition of carboxymethyl cellulose or xyloglucan to the culture medium reduces formation of the I_α phase, increasing the I_β fraction; according to an electron-microscopic examination, this is associated with a decrease in the width of CAX microfibrils. Similar effects have also been observed by other authors [23] upon introduction of oligo- and polysaccharides into the culture medium. Samples of CAX and its composites have been prepared under various synthesis conditions with addition of lignin–carbohydrate complexes or specific polysaccharides to the culture medium; an X-ray diffraction study of these samples has shown that some additives increase the content of the I_β phase, and, in some cases, the crystal structure does not change (the I_α phase remains) or low-crystalline composites are obtained [23].

Our goal was to reveal a correlation between the structural organization of CAX macrochains in the course of the syntheses, suggested in [3] (Fig. 1), and structural parameters of cellulose macrosamples in the course of drying of CAX gel films. Here, we report the results of optimization of the CAX synthesis by the VKM V-880 *A. xylinum* strain and the structural features of CAX samples, which were evaluated by X-ray diffraction analysis and dielectric spectroscopy.

EXPERIMENTAL

The cellulose synthesis by the VKM V-880 *A. xylinum* strain maintained at the Microbiology Chair, St. Petersburg State University, was performed in a culture medium containing aqueous solutions of yeast extract (YE), glucose, peptone, ethanol, and

wort in optimized concentrations, at pH 5.9–6.0. The seed was a 48-h *A. xylinum* culture grown in a medium containing YE and wort (6° Baling scale) in 1 : 1 ratio, with 2 wt % glucose and 1 vol % ethanol. Cultivation was performed at 29–30°C for 6–7 days, after which CAX was separated and intermittently washed with boiling 0.5–1% aqueous NaOH to remove *A. xylinum* cells. Then CAX was washed to remove NaOH with distilled water, 0.5% acetic acid solution, and again distilled water to neutral reaction. The resulting CAX was stored either as a gel film (in distilled water at 5°C) or (after autoclave sterilization) at room temperature, or it was dried in a vacuum at 40°C and stored in the dry state. The procedure was optimized by additive-lattice experimental design [24]; the five varied factors were concentrations of the components of the medium, and the cellulose yield was determined at different factor values.

X-ray diffraction patterns (DRON-2 diffractometer and RKV-86 X-ray camera, Ni-filtered Cu_{K_α} radiation) were measured for the initial CAX gel films cleaned to remove the culture medium, and also for the films from which a certain amount of water was removed (before and after drying in air at room temperature to the air-dry state). The dielectric properties of CAX were measured with a TR-9701 device in the frequency range 1–100 kHz at temperatures from –140 to 120°C. A two-electrode cell with chrome-plated brass electrodes and Teflon insulation was used. The measurements were performed in dry air with 30–60-μm-thick film samples dried in a vacuum at 60°C.

It is known that *A. xylinum* well develops in culture media containing glucose and some other monosaccharides as carbon sources, and also yeast extract as growth factor and source of nitrogen [25]. To determine the cellulose-producing power of the VKM V-880 *A. xylinum* strain, the culture medium based on the initial medium containing glucose, YE, and peptone was optimized. The effect of organic additives, wort and ethanol, on the biosynthesis of cellulose was elucidated [26]. Determination of the cellulose yield from culture media of 25 different compositions showed that, at the optimal combination of the components (7 wt % glucose, 0.3 wt % YE, 30 vol % wort, 0.3 wt % peptone, 3 vol % ethanol), up to 50 g of air-dry cellulose is obtained from 1 m^2 of the reactor surface.

It has been found previously that CAX can be synthesized on culture media with various cheap sources of carbon: industrial wood hydrolyzates, peat hydrolyzates, molasses, and other media containing monosaccharides [27, 28]. To determine the structural characteristics of CAX synthesized by the VKM V-880 strain, we used gel films prepared in a medium containing 2% glucose, 0.2% peptone, 0.3% YE, and 2 vol % ethanol. The IR absorption bands and X-ray reflections of these samples were found in the ranges characteristic of cellulose I. Determination of the molecular weight of CAX by sedimentation and diffusion in cadoxen gave an M_{SD} value of 5×10^5. The polydispersity index M_z/M_w determined by correlation laser spectroscopy in cadoxen [26] was approximately 1.1. All these data are nicely consistent with the CAX characteristics available from the literature [29].

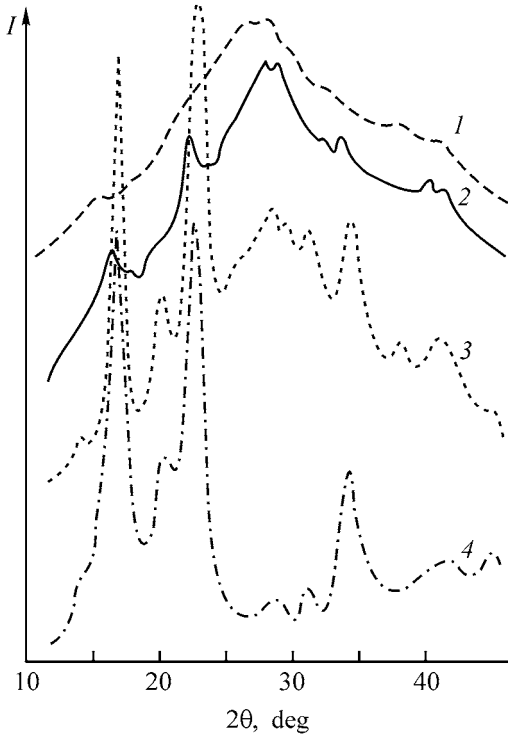

Fig. 2. Diffraction patterns of CAX in various steps of gel film drying. (*I*) Intensity and (2θ) Bragg angle; the same for Figs. 4–6. (*1*) Initial gel films with the dry polymer : water ratio of 1 : 100; (*2*) CAX sample squeezed to remove 50% of water; (*3*) sample dried at 20°C for 3 h; (*4*) sample dried in a vacuum at 40°C.

Since the X-ray diffraction patterns obtained from CAX gel films dried under various conditions differed from those reported in [23, 30], it seemed appropriate to study in more detail the kinetics of water removal from the CAX gel film in the course of drying.

The diffraction pattern of the initial gel film with the dry polymer : water ratio of 1 : 100 (Fig. 2, curve *1*) is characterized by a broad maximum at 2θ =

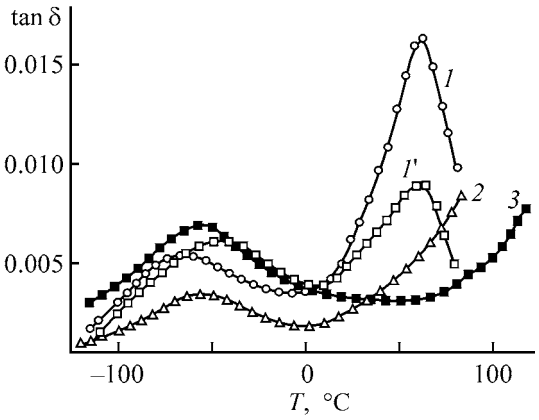

Fig. 3. Temperature dependence of the dielectric loss tangent tan δ for (*1*, *1*') CAX, (*2*) CAX heated to 100°C in a vacuum in the course of measurement, and (*3*) dried cotton linter. Measurement frequency, kHz: (*1–3*) 1 and (*1*') 10.

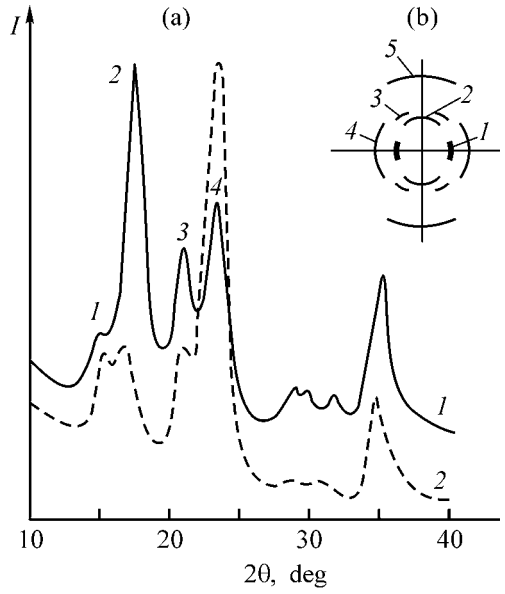

Fig. 4. (a) Diffraction patterns and (b) scheme of X-ray pattern obtained at (a) perpendicular and (b) parallel incidence of the X-ray beam relative to the plane of the dry sample. Sample: (a) (*1*) CAX and (*2*) LC; (b) CAX.

20°–40°. When 40–50% of the initial water is removed from the gel film, clear reflections appear against the background of this halo at 2θ 15°–16°, 23°, 27°, 32°–34°, and 40°–42°, with the broad maximum in the range 25°–30° being preserved (Fig. 2, curve *2*). After drying this sample in air at 20°C for 2–3 h, the reflection positions and intensities changed (Fig. 2, curve *3*). A noticeable diffuse background remained in the range 2θ = 20°–40°, and the reflections corresponding to *d* 0.532, 0.435, 0.390, and 0.259 nm became the strongest. In the X-ray patterns of the CAX films dried in a vacuum at 40°C (Fig. 2, curve *4*), the positions of these four reflections remained unchanged, whereas the diffuse halo virtually disappeared.

However, the samples dried under these conditions still contained water molecules, as suggested by the CAX relaxation properties determined by dielectric spectroscopy [31]. Figure 3 shows the temperature dependence of the dielectric loss tangent, $\tan\delta = f(T)$, for samples of CAX and, for comparison, cotton linter cellulose (LC). For samples of both CAX and LC, $\tan\delta_m$ passes through a maximum at negative temperatures (about –60°C, 1 kHz). According to the concept of the relaxation properties of cellulose [31–33], this range of dielectric loss in CAX must be associated with relaxation of the dipole polarization and mobility of primary hydroxy groups of cellulose molecules. Above 0°C, the dielectric loss increases. At 60–70°C, the loss decreases irrespective of the measurement frequency (curves *1*, *1*'); heating in a vacuum enhances this trend (curves *1*, *2*). This fact suggests removal of compounds increasing the electrical conductivity from the sample bulk (in the given case, this is, most probably, water [33]).

Simultaneoulsy, $\tan\delta_m$ decreases, and the maximum shifts from –60°C to higher temperatures. This suggests disappearance of the plasticization effect associated with the presence of water molecules forming hydrogen bonds with primary hydroxyls. The break-down of the hydroxyl–water complexes does not cause the peak of $\tan\delta_m$ to grow in intensity, which may be due to involvement of the released OH groups in a new system of intermolecular hydrogen bonds. Comparison of the dependences $\tan\delta = f(T)$ for CAX and LC samples (Fig. 3, curves *2*, *3*) shows that the maximal value of $\tan\delta_m$ at –60°C for CAX is two–three times lower than for LC. Since the height of the peak at –60°C is determined by the amount of primary OH groups that can participate in thermal motion and this motion can occur in defective areas only, it can be presumed that bacterial cellulose, compared to linter cellulose, is characterized by a more regular network of hydrogen bonds and a more regular structure [31–33]. Indeed, the X-ray diffraction patterns of CAX and LC samples showed that CAX films were more ordered (Fig. 4a, curve *1*); all the reflections of CAX were indexed in the monoclinic system of modification I, which is a two-phase system of CI_α and CI_β.

Particular attention should be given to the range 2θ = 13°–18° in the diffraction pattern of CAX. It is seen that the $\bar{1}10$ reflection (2θ = 15°) of the CAX

film (Fig. 4a, curve *1*) is considerably weaker as compared to LC (Fig. 4a, curve *2*). At the same time, the intensity of the reflection at $2\theta = 16°50'$ [sum of (110) and (002) reflections] is many times higher as compared to LC and varies from one sample to another.

To reveal a planar texture in CAX films, we measured the X-ray patterns with the plane of the dried sample arranged in parallel with the incident X-ray beam. Figure 4b shows the scheme of the five major reflections of CAX, denoted by the corresponding numerals in Fig. 4a.

We revealed an appreciable redistribution of the reflection positions and intensities. A reflection with $d = 0.607$ nm ($2\theta = 15°$), corresponding to the reflection from the $\bar{1}10$ planes, is clearly seen in the equatorial region. A reflection in the meridional region at $d = 0.523$ nm [reflection from the (002) planes] is clearly seen against the background of a weak ring reflection at $2\theta = 17°$. The (110) reflection in the equator is absent; only a weak "ring" reflection from (110) planes with $d = 0.532–0.535$ nm is observed.

As for the other reflections, the weak third reflection at $2\theta = 20°40'$ is detected in the vicinity of the meridional region and is undoubtedly a sum of reflections from the (102) and (012) planes of the monoclinic lattice with $d = 0.437$ and $d = 0.432$ nm. In the equatorial region, there is a fairly strong fourth reflection with $d = 0.389–0.392$ nm, corresponding to the reflections from the (200) planes in which hydrogen-bonded cellulose chain molecules are arranged to form parallel layers. Finally, the fifth reflection with $d = 0.259–0.260$ nm, which is a superposition of moderately strong reflections from the system of planes (004), (220), (031), and (023), is clearly seen in the meridional region of the X-ray pattern of a CAX film taken from the end side, i.e., it characterizes the periodicity along the polymeric chain.

Thus, aggregates of CAX microfibrils are arranged in the plane of the dried film, forming an axial texture whose axis is perpendicular to the film plane. Since the (110) reflection ($2\theta = 15°$) is only manifested in the majority of samples when the X-ray beam is parallel to the sample surface, it can be concluded that, in the crystallites constituting CAX ribbons, the $(\bar{1}10)$ planes of the monoclinic cell are arranged parallel to the macrosample, i.e., an axial-planar texture arises [34].

Comparison of the diffraction patterns of CAX films (VKM V-880 strain) prepared in this study and CAX samples produced by the ATCC 53524 strain

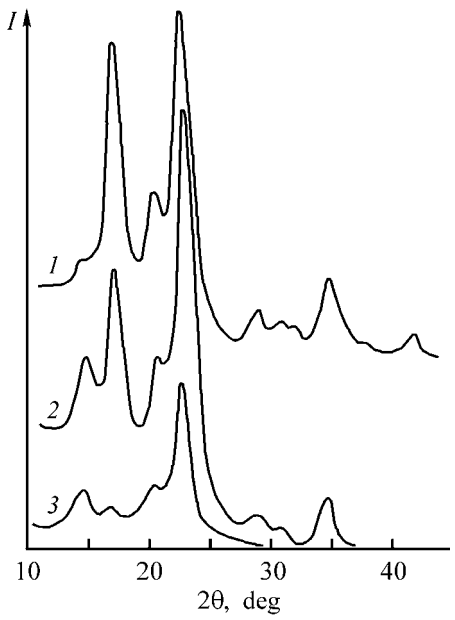

Fig. 5. Diffraction patterns of CAX samples dried (*1*) at 40°C and (*2*) lyophilically after freezing the gel film at –30°C; (*3*) CAX sample (ATCC 53524 strain) dried in the course of freezing [23].

[23] reveals differences in the intensities of some reflections (Fig. 5). This may be due to different procedures of sample preparation. The films were dried on glass supports at room temperature or at 40°C in a vacuum; they had an axial-planar texture. The CAX sample dried in the course of freezing [23] had an isotropic polycrystalline structure (Fig. 5, curve *1*). To eliminate the texturing effect, we changed the drying procedure: A gel film was first frozen at –30°C and then dried lyophilically. However, after such a treatment, the axial-planar texture of the CAX film was preserved, even though to a considerably lesser extent (Fig. 5, curve *2*).

The use of isotropic polycrystalline samples for X-ray diffraction analysis allowed resolution of reflections at 2θ 15° and 17° and their assignment to the I_α and I_β modifications [23]. For the textured samples under consideration, this is impossible. However, the presence of the (002) reflection on the meridian of the diffraction pattern (Fig. 4b) obtained at parallel arrangement of the CAX sample plane relative to the incident X-ray beam indicates that the gel film contains an appreciable amount of the monoclinic I_β phase with the parameters $a = 0.801$, $b = 0.817$, $c = 1.036$ nm (macromolecular axis), and $\beta = 97°$, suggested in [10].

The diffraction patterns of CAX films prepared using, in the biosynthesis step, such carbon sources as industrial hydrolyzates of wood, peat, and liquors

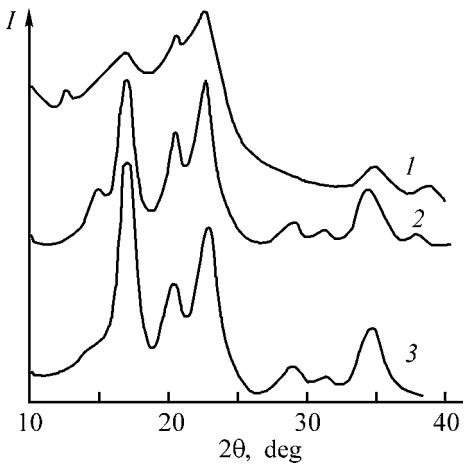

Fig. 6. Diffraction patterns of CAX samples prepared using different carbon sources. Medium: (*1*) containing wood hydrolyzate, (*2*) standard [26], and (*3*) containing glycerol.

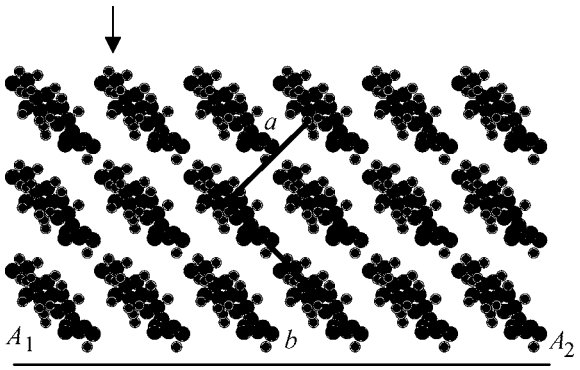

Fig. 7. Model of cellulose chain packing (projection onto the *ab* plane) in the monoclinic cell. (A_1–A_2) Orientation of ribbon microfibrils in the macrofilm plane. The arrow shows the direction of mini-sheets in the course of biosynthesis.

from pulp-and-paper and fruit-and-berry productions [27, 28] show that, depending on conditions of cultivating *A. xylinum*, the CAX produced does not always have the cellulose I structure (Fig. 6, curve *2*); in some cases, it is a mixture of the cellulose I and cellulose II modifications (Fig. 6, curve *1*). The biosynthesis conditions also govern the extent of microfibril orientation in the plane of the CAX film. For example, using glycerol as the carbon source, we observed in CAX samples a clear axial-planar texture (Fig. 6, curve *3*).

Thus, comparison of the diffraction patterns of the CAX gel films dried by different procedures or prepared under different cultivation conditions with the data given in [23, 30] shows that, under conditions of our experiments, a texturing effect arises. Furthermore, the previously published electron diffraction data [35] in combination with the X-ray diffraction patterns for CAX of the VKM V-880 strain suggest that, in the textured samples, the content of the I_β modification exceeds that of the I_α modification.

The possibility of obtaining different I_α/I_β ratios in CAX ribbon formations depending on the conditions of cultivating *A. xylinum* was discussed in [15, 23]. These papers consider the shear stresses in thin planar ribbon ensembles of CAX in the course of simultaneous crystallization and twisting. The ribbons are twisted owing to rotation of bacteria during their forward motion in a culture medium. Aggregation of microfibrils yields wide (40–60 nm) ribbons; their twisting gives rise to end stresses, inducing formation of the I_α structure. On the contrary, the I_β structure is formed in the central parts of the ribbons. If the ribbons are less twisted or microfibrils have smaller transverse size, the number of the stressed regions is considerably smaller, which favors formation of the I_β structure in CAX. Bowling *et al.* [36] observed untwisting of CAX ribbons during degradation of cellulose chains effected by fungus cellulases. This rotary motion was explained by lifting of bending stress and formation of relaxing conformations.

Presumably, in our case the CAX ribbons, orienting on the surface of the culture medium, form a network of hydrogen bonds via primary hydroxy groups, which can prevent twisting of ribbon ensembles and result in a higher content of the I_β structure, compared to I_α, in textured CAX samples.

Proceeding with the concept suggested in [4], we propose a model of cellulose chain packing in the projection onto the *ab* plane for the monoclinic cell with two macromolecules (Fig. 7). The A_1–A_2 line denotes the directing defining the orientation of microfibrillar ribbons on the surface of the culture medium. Such an orientation of glucoside fragments on the microfibril surface explains the presence of a large amount of water molecules hydrogen-bonded with primary hydroxyls. As seen from Fig. 7, the C^6–OH groups are arranged at the phase boundary along the A_1–A_2 line; according to the theoretical calculations [6], these groups have the *tg* conformation in the triclinic I_α structure and the *gt* conformation in the monoclinic structure, participating in the latter case in the hydrogen bonding between the mini-layers. The direction of mini-layers (this concept was suggested in [3]; Fig. 1) is marked in the scheme with an arrow. It is seen (Fig. 7) that the mini-layers are perpendicular to the culture medium surface.

It is known that CAX gel films can retain from 100 to 200 g of water per gram of dry polymer, preserving

a high intrinsic tensile strength (up to 2 kgf mm^{-2}) [26]. The X-ray patterns suggest that the microfibrillar ribbons oriented on the film surface act not only as a reinforcing network but also as hydrophilic layers capable of interacting with a large amount of water molecules. According to electron-microscopic data [35], the diameter of the aggregates is about 50 nm, and their length is extremely large. Microfibrillar aggregates occupy an insignificant part of the gel film volume, which allows introduction depending on the degree of film drying, of diverse systems into gel films. For example, it has been shown that a CAX gel film is an excellent carrier of such antiseptics as Catapol and Poviargol containing silver clusters [37, 38].

CONCLUSIONS

(1) The composition of the culture medium was optimized with the aim to attain the maximal yield of cellulose produced by *Acetobacter xylinum*. The VKM V-880 strain of *A. xylinum* is capable of synthesizing high-molecular-weight cellulose in a static culture using a wide range of carbon sources.

(2) The kinetics of structural transformations that occur in this cellulose when water is removed from gel films in the course of drying was studied by X-ray diffraction and dielectric spectroscopy. It was shown that, in the dried films of highly crystalline cellulose, an axial-planar texture is formed in which crystallographic planes ($\bar{1}10$) of the monoclinic cell (d = 0.61 nm) are arranged parallel to the sample plane.

(3) To describe the packing of ribbon aggregates in the plane of a cellulose film, a model was suggested according to which the mini-sheets constituting the aggregates are arranged in the perpendicular direction relative to the phase boundary between the culture medium and air.

ACKNOWLEDGMENTS

The study was supported financially by the Russian Foundation for Basic Research (project no. 01-03-33158) and NWO (grant no. 047.009.015).

REFERENCES

1. Delmer, D.P., *Ann. Rev. Plant Physiol. Plant Mol. Biol.*, 1999, vol. 50, pp. 245–276.
2. Brown, R.M., Jr. and Saxena, J.M., *Plant Physiol. Biochem.*, 2000, vol. 38, nos. 1/2, pp. 57–67.
3. Brown, R.M., Jr., *J.M.S.–Pure Appl. Chem.*, 1996, vol. 33A, no. 10, pp. 1345–1373.
4. Ranby, B., *Cellulose Chem. Technol.*, 1997, vol. 31, pp. 3–16.
5. O'Sullivan, A.C., *Cellulose*, 1997, vol. 4, pp. 173–207.
6. Vietor, R.J., Mazeau, K., Lakin, M., and Perez, S., *Biopolymer*, 2000, vol. 54, pp. 342–354.
7. Wada, M., Okano, T., and Sugiyama, J., *Cellulose*, 1997, vol. 4, pp. 221–232.
8. Wada, M., Okano, T., and Sugiyama, J., *J. Wood Sci.*, 2001, vol. 47, pp. 124–128.
9. Debzi, E.M., Chanzy, H., Sugiyama, J., *et al.*, *Macromolecules*, 1991, vol. 24, no. 25, pp. 6816–6822.
10. Sugiyama, J., Young, R., and Chanzy, H., *Macromolecules*, 1991, vol. 24, no. 14, pp. 4168–4175.
11. Cousins, S.K. and Brown, R.M., Jr., *Polymer*, 1997, vol. 38, no. 4, pp. 897–912.
12. Yamamoto, H. and Horii, F., *Macromolecules*, 1993, vol. 26, no. 6, pp. 1313–1317.
13. Sassi, J.-F., Tekely, P., and Chanzy, H., *Cellulose*, 2000, vol. 7, pp. 119–132.
14. Wada, M. and Okano, T., *Cellulose*, 2001, vol. 8, pp. 183–188.
15. Baker, A.A., Helbert, W., Sugiyama, J., and Miles, M.J., *Biophys. J.*, 2000, vol. 79, pp. 1139–1145.
16. Hirai, A. and Horii, F., *JCR Annual Rep.*, 1999, vol. 6, pp. 28–29.
17. US Patent 4655758.
18. EP Patent O 197748 B1.
19. Yamanaka, S., Ishihara, M., and Sugiyama, J., *Cellulose*, 2000, vol. 7, pp. 213–225.
20. Yamamoto, H., and Horii, F., *Cellulose*, 1994, vol. 1, pp. 57–66.
21. Yamamoto, H., Horii, F., and Hirai, A., *Cellulose*, 1996, vol. 3, pp. 229–242.
22. Hirai, A., Tsuji, M., Yamamoto, H., and Horii, F., *Cellulose*, 1998, vol. 5, pp. 201–213.
23. Iwata, T., Indrarti, L., and Azuma, J.-I., *Cellulose*, 1998, vol. 5, pp. 215–228.
24. Biryukov, V.V., Kantere, V.M., in *Optimizatsiya periodicheskikh protsessov mikrobiologicheskogo sinteza* (Optimization of Batch Processes of Microbiological Synthesis), Moscow: Nauka, 1985, ch. 3, pp. 18–54.
25. Whister, R.L., in *Methods in Carbohydrate Chemistry*, vol. 3: *Cellulose*, New York: Academic, 1963, pp. 4–9.
26. Khripunov, A.K., Tkachenko, A.A., Moskvicheva, Yu.B., *et al.*, in *Biotekhnologiya i genetika: Mezhvuzovzkii sbornik nauchnykh trudov* (Biotechnology and Genetics: Intercollegiate Coll. of Scientific Works), Nizhni Novgorod: Nizhegorod. Gos. Univ., 1991, pp. 54–64.
27. RF Patent 2141530.
28. RF Patent 2189394.

29. Nevell, T.P. and Zeronian, S.H., in *Cellulose Chemistry and Its Application*, New York: Ellis Horwood, 1985, pp. 67–73.
30. Watanabe, K., Tabuchi, M., Morinaga, Y., and Yoshinaga, F., *Cellulose*, 1998, vol. 5, pp. 187–200.
31. Gladchenko, S.V., Khripunov, A.K., Tkachenko, A.A., and Borisova, T.I., Abstracts of Papers, *II Mezhdunarodnyi simpozium "Stroenie, svoistva i kachestvo drevesiny"* (II Int. Symp. "Structure, Properties, and Quality of Wood"), Moscow–Mytishchi, October 21–24, 1996, p. 48.
32. Borisova, T.I., Petropavlovskii, G.A., and Kotel'nikova, N.E., *Vysokomol. Soedin., Ser. A*, 1979, vol. 21, no. 9, pp. 2031–2037.
33. Gladchenko, S.V., Borisova, T.I., Larina, E.I., and Petropavlovskii, G.A., *Vysokomol. Soedin., Ser. B*, 1992, vol. 34, no. 3, pp. 21–23.
34. Tsvankin, D.Ya., *Vysokomol. Soedin.*, 1963, vol. 5, no. 1, pp. 123–128.
35. Zanaveskina, I.S., Stiopina, N.D., Khripunov, A.K., *et al.*, Abstracts of Papers, *8th European Conf. on Organized Films*, Otranto (Italy), September 3–7, 2001, paper 11.12.
36. Bowling, A.J., Amano, Y., Lindstron, R., and Brown, R.M., Jr., *Cellulose*, 2001, vol. 8, no. 1, pp. 91–97.
37. Kopeikin, V.V. and Panarin, E.F., *Dokl. Ross. Akad. Nauk*, 2001, vol. 380, no. 4, pp. 497–500.
38. Khripunov, A.K., Tkachenko, A.A., Baklagina, Yu.G., *et al.*, *II Mezhdunaropdnaya konferentsiya "Sovremennye podkhody k razrabotke effektivnykh perevyazochnykh sredstv, shovnykh materialov i polimernykh implantantov": Materialy konferentsii* (Proc. II Int. Conf. "Modern Approaches to Development of Effective Dressings, Suture Materials, and Polymeric Implantants"), Moscow: November 21–22, 1995, pp. 71–73.